Heliyon 10 (2024) e25620

Contents lists available at ScienceDirect

Heliyon

journal homepage: www.cell.com/heliyon

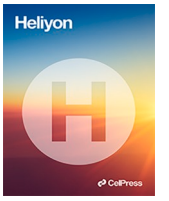

Research article

Effect of cooking on structural changes in the common black bean (*Phaseolus vulgaris* var. Jamapa)

Madeleine Perucini-Avendaño [a], Israel Arzate-Vázquez [b], María de Jesús Perea-Flores [b], Daniel Tapia-Maruri [c], Juan Vicente Méndez-Méndez [b], Mayra Nicolás-García [a,d], Gloria Dávila-Ortiz [a,*]

[a] *Departamento de Ingeniería Bioquímica, Escuela Nacional de Ciencias Biológicas, Instituto Politécnico Nacional (IPN), Av. Wilfrido Massieu S/N, Unidad Profesional Adolfo López Mateos, Zacatenco, Delegación Gustavo A. Madero, 07738, Mexico City, Mexico*

[b] *Centro de Nanociencias y Micro y Nanotecnologías, Instituto Politécnico Nacional (IPN), Av. Luis Enrique Erro S/N, Unidad Profesional Adolfo López Mateos, Zacatenco, Delegación Gustavo A. Madero, 07738, Mexico City, Mexico*

[c] *Centro de Desarrollo de Productos Bióticos-Instituto Politécnico Nacional, Carretera Yautepec-Jojutla Km. 6, Calle CEPROBI No. 8, Col. San Isidro, Yautepec, C.P. 62731, Morelos, Mexico*

[d] *Tecnológico Nacional de México/ITS de Teziutlán, Ingeniería en Industrias Alimentarias, Fracción I y II, Aire Libre S/N, 73960, Teziutlán, Puebla, Mexico*

A R T I C L E I N F O

Keywords:
Black bean
Seed coat
Cooking process
Microstructural analysis
Proximate analysis
Image analysis

A B S T R A C T

The cooking process is fundamental for bean consumption and to increase the bioavailability of its nutritional components. The study aimed to determine the effect of cooking on bean seed coat through morphological analyses with different microscopy techniques and image analyses. The chemical composition and physical properties of raw black bean (RBB) and cooked black bean (CBB) seeds were determined. The surface and cross-sectional samples were studied by Optical microscopy (OM), environmental scanning electron microscopy (ESEM), atomic force microscopy (AFM) and confocal laser scanning microscopy (CLSM). The composition of samples showed significant differences after the cooking process. OM images and gray level co-occurrence matrix algorithm (GLCM) analysis indicated that cuticle-deposited minerals significantly influence texture parameters. Seed coat surface ESEM images showed cluster cracking. Texture fractal dimension and lacunarity parameters were effective in quantitatively assessing cracks on CBB. AFM results showed arithmetic average roughness (R_a) (121.67 nm) and quadratic average roughness (R_q) (149.94 nm). The cross-sectional ESEM images showed a decrease in seed coat thickness. The CLSM results showed an increased availability of lipids along the different multilayer tissues in CBB. The results generated from this research work offer a valuable potential to carry out a strict control of bean seed cooking at industrial level, since the structural changes and biochemical components (cell wall, lipids and protein bodies) that occur in the different tissues of the seed are able to migrate from the inside to the outside through the cracks generated in the multilayer structure that are evidenced by the microscopic techniques used.

* Corresponding author. Departamento de Ingeniería Bioquímica, Escuela Nacional de Ciencias Biológicas, Instituto Politécnico Nacional (IPN), Av. Wilfrido Massieu s/n, Unidad Profesional Adolfo López Mateos, Zacatenco, Delegación Gustavo A. Madero, C.P. 07738, Mexico City, Mexico.

E-mail addresses: madeleineperucini@gmail.com (M. Perucini-Avendaño), iarzate@ipn.mx (I. Arzate-Vázquez), peflo_ma@hotmail.com (M.J. Perea-Flores), dmaruri@ipn.mx (D. Tapia-Maruri), jmendezm@ipn.mx (J.V. Méndez-Méndez), mayra.ng@teziutlan.tecnm.mx (M. Nicolás-García), gdavilao@yahoo.com (G. Dávila-Ortiz).

https://doi.org/10.1016/j.heliyon.2024.e25620
Received 16 May 2023; Received in revised form 29 January 2024; Accepted 31 January 2024
Available online 8 February 2024

1. Introduction

The common bean (*Phaseolus vulgaris* L.) is one of the most important foods in the Mexican culture since Prehispanic times due to its nutritional attributes as an excellent source of protein, fiber, calcium, and iron [1]. Likewise, its biological activity has been demonstrated as antioxidant, anticancerigenous, anti-diabetic, and as a weight control [2–4].

Structurally, beans are composed of two main tissues: seed coat and endosperm [5,6]. The seed coat is the outer covering of the seed, and the endosperm is the most abundant tissue that contains mainly proteins, lipids (a good source of poly unsaturated fatty acids with functions of peroxidation reactions), and carbohydrates (reserve and structural) [7–9]. The seed coat acts as a barrier for the endosperm against different environmental conditions, it is a thin and resistant layer due to its microstructure and composition. The presence of calcium oxalate crystals has been evidenced, which intervene in the mechanical and textural properties [10–13]. On the other hand, the color depends on the presence of phenolic compounds in the seed [1,3,12,14,15].

In the surface of the seed coat, there is a small opening called a micropyle, which is the structure through which water penetrates to begin the germination process [16,17]. The architecture of the seed coat is described as a multilayered structure; the first tissue covering the whole seed is called the cuticle, followed by palisade cells of elongated sclereids called macrosclereids, and, finally, the parenchyma cells (nutrient transport layer during the development of the seed) [18,19].

All commercial varieties of beans are subjected to a cooking process before being consumed. This treatment increases the digestibility of the starch and modifies nutritional components, such as proteins. Macroscopic texture changes during thermal processing of black bean seeds involve hydration, solubilization, swelling of the starch granules, and dissolution of the cell wall and the lamellar polymers of the cotyledon [20,21].

The studies carried out so far regarding the effect of the cooking process on beans have focused mainly on the endosperm, particularly, the starch granules of hardened beans [22] grown under different water regimes [9], and on bean flour by studying the nutritional and non-nutritional compounds. These studies have provided information at the microstructural level of the endosperm after the cooking process through the use of microscopic techniques; however, a global study on structural changes in the bean seeds has not been performed yet. Studying the microstructure of the bean seed will allow evaluating how the cooking process influences its nutritional properties (protein denaturation, starch gelatinization, and inactivation of non-nutritional compounds) and texture properties, which affect the technological processes (delaying, accelerating, and optimizing the quality of the cooking process).

Microscopy techniques are valuable tools to study the microstructure of food matrices, as well as the distribution of phenolic compounds, proteins, and carbohydrates. Several authors [23–25] have reported the use of image analysis combined with microscopy techniques, demonstrating their effectiveness in the measurement of morphological, morphometric, and textural characteristics using algorithms such as GLCM [13,21,24,26,27]. The objective of this work was to study the microstructural changes that occur in the black bean (*Phaseolus vulgaris* L.) during the cooking process using microscopy techniques combined with image analysis.

2. Materials and methods

2.1. Plant material

Twenty kilograms of raw black bean (RBB) seeds of the Jamapa variety were procured from *Campo Experimental Cotaxtla* of Instituto Nacional de Investigaciones Forestales, Agrícolas y Pecuarias (INIFAP) and the Schettino Company of the state of Veracruz, Mexico. RBB seeds were manually cleaned to remove seeds with cracks or appreciable damaged seeds and stored at room temperature for later use. The moisture content of RBB was 8.57 ± 0.13% dry weight (DW), which is within the range reported by Corzo-Rios et al. [28] (<15%).

2.2. Cooking process

Beans were cooked following the method of Dueñas et al. [29] with the following modifications. RBB seeds were placed in distilled water a 1:3 w/v ratio in a pressure cooker at 100 °C, for a period of 55 min, which was defined until 75% of the beans felt soft and slightly lumpy [30]. Finally, CBB seeds were separated for further analysis.

2.3. Proximal chemical composition

RBB and CBB were lyophilized in a freeze dryer (FreeZone 2.5, Labconco, Kansas City, MO, USA) and pulverized using a mechanical mill (M 20, IKA, Germany). Methods from the Association of Official Analytical Chemists [31] were used to analyze the following parameters: ash content (method 923.03), protein (NX6.25, method 955.04), Lipid content crude fat (method 920.39), and total carbohydrate contents were estimated by the formula (% total carbohydrates = 100 - % protein - % ash - % Lipid content crude fat). All reported proximate analysis data in this manuscript are the arithmetic mean of triplicate measurements.

2.4. Microstructural analysis of RBB and CBB

The chemical and microstructural analyses of the seeds are relevant aspects for the knowledge of their properties and function [21]. In this research, we analyzed the surface of the seeds corresponding to the external part of the seed coat and the different tissues

present in the beans' cross-section, corresponding to the seed coat and cotyledon. Microscopy techniques have also been useful to study the architecture, microstructure (OM, ESEM, AFM), and macromolecules distribution (CLSM) in bean seeds.

2.4.1. Optical microscopy

Texture image analysis was performed to study changes in the seed coat surface after the cooking process (RBB and CBB) using the images from an optical microscope (BX-41, OLYMPUS, Japan). The images were acquired in bright-field in TIFF format with a size of 1280 × 1024 pixels using the NIS-Elements software (V.2.30).

2.4.2. Environmental scanning electron microscopy

The microstructure of the surface and cross-section seed coat of RBB and CBB were observed using an ESEM (EVO LS10, Carl Zeiss, Germany). The samples were placed on aluminum stubs attached with double-sided carbon conductive tape; the images were acquired with a secondary electron detector at 20 kV [32]. Additionally, elemental microanalysis of the seed coat surface and cross-section were determined with the coupled energy-dispersive X-ray detector (EDX) [33]; this analysis allowed the characterization of the crystals by cross-section.

2.4.3. Atomic force microscopy

Seed coat surface roughness of the RBB and CBB was analyzed through AFM. The samples were placed on stainless steel disc with double-sided adhesive tape. Three different areas (2.5 × 2.5 μm^2, 1 × 1 μm^2 and 820 × 820 nm^2) were scanned in the tapping mode (RTESP-300, Bruker, Camarillo, CA) at 1.0 Hz applying an AFM (MultiMode V connected to minicontroller NanoScope V, Bruker, USA). The micrographs were processed with the software NanoScope Analysis v. 1.80 (Veeco, USA), to calculate the roughness parameters R_a and R_q [34]. All images were stored in RGB color format (704 × 576 pixels) in TIFF format.

2.4.4. Confocal laser scanning microscopy

Confocal Laser Scanning Microscopy is used to visualize the different structures of tissues in combination with multicolor fluorescent staining and labeling of sample structures of interest based on their composition [35]. For the histological study, cross-sections of the RBB samples were softened and fixed with a saturated solution of picric acid for 5 h [36,37] and washed with 70% ethanol to eliminate the acid traces. After that, the sections were dehydrated in a gradual series of ethyl alcohol solutions (80, 90, and 100%) for 2 h each one [36]. After this treatment, the RBB samples were subsequently cleared with ethanol-xylol series (3:1, 1:1, 1:3) and absolute xylol for 10 min. The samples were embedded in paraffin-xylol (3:1) for 4 h at 60 °C and Paraplast® (absolute paraffin) (SIGMA Chemical Co., St. Louis, MO, USA) in a tissue embedding system (KD-BM-II, Kedee Instrument, Co., LTD. Jinhua, China). On the other hand, dehydration of the CBB samples was carried out with 30, 40, 50, 60, 70, 80, 90, 100% ethanol, and clarification was conducted with the same ethanol-xylol series for 5 min. Finally, the CBB samples were embedded in the same way as the RBB samples. To obtain 10-μm thick sections, the paraffin sample blocks were cut with a rotary microtome (RM 2235, Leica Biosystems, Germany), placed in a bath with gelatin. and transferred to glass slides. Samples were deparaffinized [38] with absolute xylol, xylol-ethanol solution (1:1), and ethanol-xylol series (96, 70, and 25%) for 5 min.

The histological sections were stained with calcofluor-white (0.1%) (fluorescent, Sigma 18909, USA) for 30 min to elucidate the distribution of cell walls, which are mainly formed by polysaccharides such as cellulose and hemicellulose. Subsequently, the samples were stained with Nile red (0.1%) (fluorescent, Sigma 72485, USA) [39] for 10 min at room temperature to show the presence and distribution of the lipids in the samples. Samples were observed under the CLSM (LSM 710, NLO, Carl Zeiss, Germany) using the excitation wavelength for calcofluor-white that was 405 nm with 16% transmittance, and for Nile red that was 514 nm with 12% transmittance; then, the fluorescence in the range of 559–630 nm was detected.

2.5. Image analysis

Image analysis was used to quantify the microstructural changes generated by the cooking process. For this study, the images obtained with the techniques of light (OM and CLSM) and ESEM were analyzed by 50 measurements of each layer using ImageJ 1.52a software (National Institutes of Health, Bethesda, MD, USA, https://imagej.nih.gov/ij/).

Original images of optical microscopy were cropped (480 × 480 pixels) and processed to obtain texture image parameters for the seed coat surface of RBB and CBB. Using the GLCM algorithm, the contrast, homogeneity, and entropy parameters were obtained, as well as the distribution of minerals by 50 measurements were analyzed in each determination [21,27,40].

On the other hand, seed coat surface ESEM images were used to obtain the parameter of fractal dimension texture (FD_T) with shifting differential box counting (SDBC) and lacunarity (λ) using the box counting method with the FracLac 2015 plugins of the ImageJ software [41,42].

The morphological characterization of the CaOx crystals along the different tissues of the multilayer seed coat (number of crystals/mm^2) was carried out in the cross-section of ESEM images. For this, binary images were obtained using the threshold tool (197/255). Area (A), perimeter (P), Feret diameter, and aspect ratio (AR) parameters were obtained by 50 measurements [43]. Ninety measurements were made to obtain the average size of starch granules present in the cotyledon of the samples.

2.6. Statistical analysis

A statistical analysis was performed for all the results. Multiple comparison was made with the least significant difference (least

significant difference, LSD) of Tukey, using the MINITAB® 16 software.

3. Results and discussion

3.1. Proximal chemical composition of black beans

The chemical properties of the bean samples underwent changes during the cooking process. Table 1 shows the chemical composition, observing significant differences ($p < 0.05$) in the protein content of RBB (17.47 ± 0.05) and CBB (18.17 ± 0.05), this increase in protein content presented by CBB could be related to the interaction between phenolic compounds and proteins, which have been reported to form cross-linked complexes that undergo conformational and structural changes by the cooking process [20,44,45]. The protein content is within the range reported for different common bean varieties (17.08%–25.46%) [28,46–50], these differences in results can be explained by differences in growing conditions, including soil type, irrigation and fertilization.

In the case of lipid content, a decrease from 2.88 ± 0.11 to 2.54 ± 0.05 was observed after the cooking process, this could be attributed to a lipolysis phenomenon [51], this reaction is catalyzed in certain occasions by the high temperatures of the processing of some foods in the presence of water [28,45,52,53]. The chemical composition of these compounds changes significantly during cooking [54]. High temperatures and humidity induce lipid oxidation which can impact texture. Lipid oxidation, polymerization and degradation have been associated with the "Hard to cook (HTC)" phenomenon that directly affects macro- and micronutrient composition and, therefore, a decrease in the health benefits of bean consumption [20,45,55,56].

Significant differences were observed in the ash content of RBB (5.38 ± 0.13) and CBB (4.43 ± 0.04), this can be attributed to the solubilization and consequent outflow of these components to the cooking water. RBB showed values similar to those reported by other authors for black beans, ranging from 3.88 to 4.52% [57,58]. The CBB values are within the interval reported by Ovando-Martínez et al. [9] for different types of beans (3.96–4.65%); the mineral content depends on the residues of the extraction procedure, mineral composition of the soil which varies according to the season of the year, and the degree of maturity of the seeds [59,60].

The total carbohydrate content was determined by difference of the total chemical components on a dry basis shown in Table 1 (ash, lipids and total nitrogen). Significant differences were observed between RBB (74.27 ± 0.07) and CBB (74.86 ± 0.15) these values are within the range reported by various authors (65.4–73.4 %) [60–63]. Heat treatments increase water absorption and swelling of starch granules, breaking the bonds of amylose-amylopectin chains, starch complexes with proteins or lipids, hemicellulose, minerals, reduces antinutrients (phytic acid, tannins, and oxalates) and improves their nutritional value by increasing the digestibility of proteins and starch [9,28–30,46,64–73].

3.2. Impact of the cooking process on the microstructural properties of the seed coat surface

3.2.1. Optical microscopy

Fig. 1 shows the optical images of RBB and CBB seed coat surface. Bright areas are observed in both samples along their seed coat

Table 1
Summary of chemical composition, physical properties and crystals morphology of RBB and CBB.

Chemical composition of seed		
Compound	**RBB**	**CBB**
	g/100 g	
Proteins	17.47 ± 0.05[b]	18.17 ± 0.05[a]
Lipids	2.88 ± 0.11[a]	2.54 ± 0.05[b]
Ash	5.38 ± 0.13[a]	4.43 ± 0.04[b]
Total Carbohydrates[1]	74.27 ± 0.07[b]	74.86 ± 0.15[a]
Physical properties of seed		
Parameters		
Length (μm)	12.26 ± 0.77[b]	13.23 ± 0.96[a]
Width (μm)	8.08 ± 0.42[b]	8.28 ± 0.50[a]
Contrast	36.61 ± 6.97[a]	28.00 ± 4.77[b]
Homogeneity	0.29 ± 0.08[a]	0.34 ± 0.03[b]
Entropy	7.01 ± 0.26[a]	6.76 ± 0.18[b]
Crystal distribution (%)	1.26 ± 0.75[a]	0.26 ± 0.26[b]
Crystal morphological features		
A (μm^2)	94.45 ± 25.73[a]	17.38 ± 4.50[b]
P (μm)	58.63 ± 5.78[a]	24.83 ± 4.86[b]
Feret Diameter (μm)	16.88 ± 1.99[a]	6.77 ± 1.71[b]
AR	2.37 ± 0.477[a]	1.51 ± 0.55[a]

All results were expressed as the mean value ± standard deviation. RBB: Raw Black Bean, CBB: Cooked Black Bean, A: Area, P: perimeter. Letters between averages in the same row column indicate significant statistical differences ($p \leq 0.05$), using the Tukey test.

surface that probably correspond to randomly distributed minerals or crystals (Fig. 1a, b, d, e). The spatial distribution of bright areas was found to be random and heterogeneous throughout the cuticle tissue, and the bean seed coat has been reported to have a higher concentration of minerals compared to the cotyledon [74]. Minerals in the cuticle of the black bean seed coat can have several significant implications for seed structure, function, and potentially, its interaction with the environment. The cuticle is the protective outer layer of the seed coat, and the presence of minerals in this layer can serve several purposes (Increased mechanical strength, barrier function, resistance to environmental stress, storage of mineral nutrients, influence on seed germination, and contribution to seed coat color) [13,75–78].

The distribution of the minerals was found in a very low proportion within the material once the cooking process occurred, occupying only 0.26 ± 0.26% of the total surface area (Table 1). This finding corroborates the results obtained in the proximal chemical analysis in which the total ash content decreased once the cooking process was done, causing breakage of the granule, and lixiviation of soluble solids, minerals, and cuticle [28]. On the other hand, it provides new sensory properties, such as flavor, aroma, and texture to the seed [79], improving bioaccessibility during digestion for beneficial health effects [71].

Texture parameters based on GLCM algorithms have been effective in quantitatively characterizing microstructural changes on food surfaces [80,81]. These parameters based on the GLCM algorithms were obtained from the OM images and their values are listed in Table 1 and Fig. 1c–f. Significant differences were found in all parameters evaluated. Regarding the contrast parameter, the results showed a decrease of 26.5% after the cooking process, this behavior is associated with a considerable decrease in the content of the crystals on the surface that were solubilized. On the other hand, in CBB, we observed a slight decrease in the entropy value of the image with respect to RBB, which means that the texture of the surface of the seed coat is less disordered. This fact is again related to the content of crystals, where, due to less content of these structures, the texture of the image tends to be more homogeneous. Finally, an inverse pattern to entropy was found in the homogeneity parameter. The change in the content of the minerals located on the seed coat surface due to the cooking process notably influenced the values of the determined texture parameters.

The cooking process has an impact on the technological and functional properties that lead to the generation of new structures and biological activities. The above results indicate that the combination of OM and image analysis are essential tools for the quantitative study of the microstructure of the surface of leguminous seeds.

3.2.2. *Characterization of seed coat surface and cotyledon by means of environmental scanning electron microscopy*

ESEM images of the seed coat surface from RBB and CBB at different magnifications are shown in Fig. 2. The RBB shows irregularities along the outer layer of the seed coat that could be associated with its treatment during post-harvest handling (Fig. 2a). As observed, the cuticle (Cl) is the first tissue that presents the multilayer structure of the seed coat, which provides the bean seed with a certain impermeability to water due to its thickeness [82].

Once the cooking process was carried out, the layer covering the bean disappeared because it solubilizes. Subsequently, a cracking pattern caused by the cooking process was formed and, as a consequence, clusters of the macrosclereid cells (MC) were generated (Fig. 2b), which form the second tissue of the multilayer [82]. Fig. 2c shows that, in RBB, the MC tissue has a rough surface and is naturally compact, whereas, in CBB, the surface is fractured and cracked.

Fig. 2d shows the cracking of the seed coat surface, which caused a loss of its compact structure and exposed the individual cells of the MC. Ellipsoidal starch granules were observed on the RBB and CBB (Fig. 2e) with a size of 19–30.51 μm for raw samples and 102.3–106.8 μm after the cooking process, these starch granules which were able to migrate from the inside to the outside through the

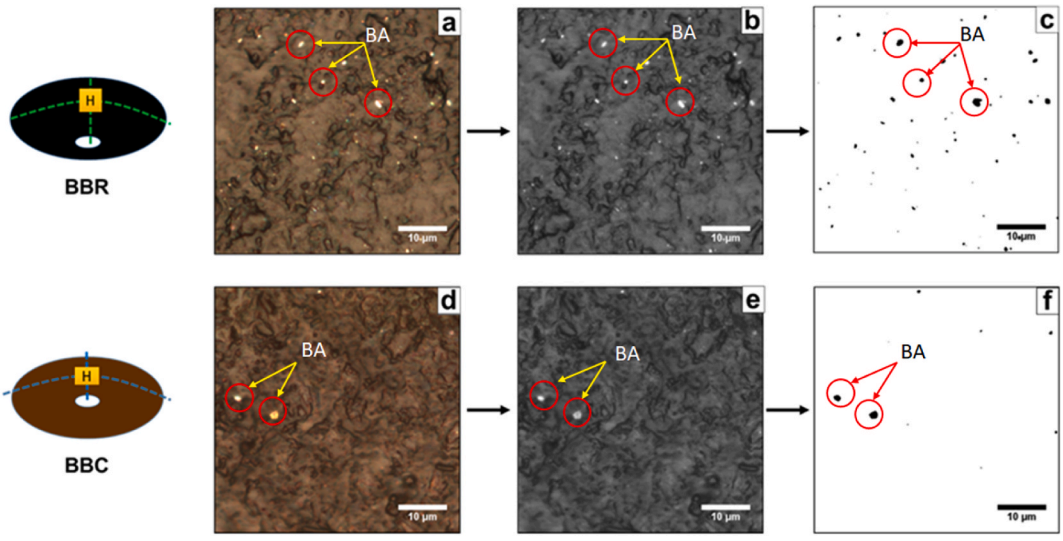

Fig. 1. Optical images of RBB (a) and CBB (d) seed coat surface at 50× resolution and their respective grayscale images (b and e) and binarized image by Image analysis (c, f).

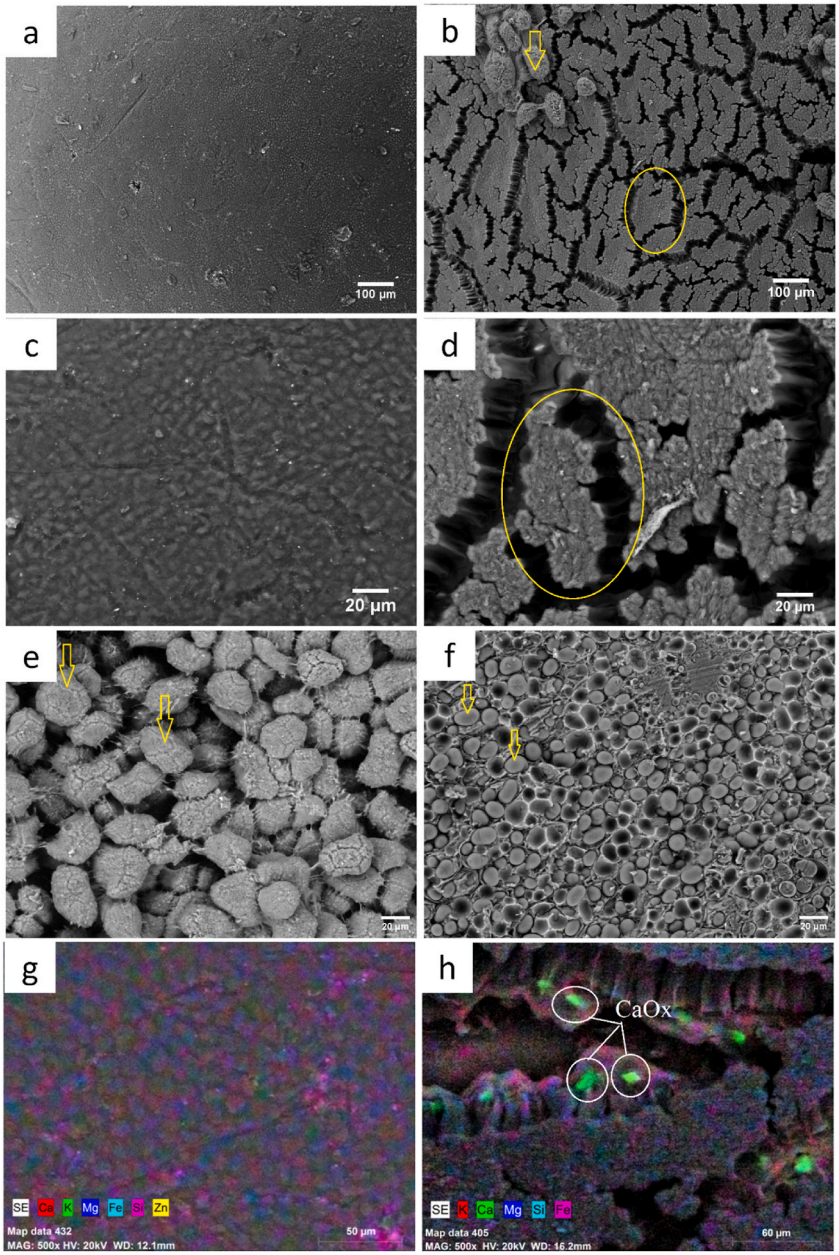

Fig. 2. ESEM images of the RBB (a) and CBB (b) surface at 100×, and their respective magnifications at 500× (c) and (d), EDS spectrum of the RBB and CBB surface (d) and (e).

cracks generated in the multilayer structure. These structural changes will be taken up again in the CLSM section for a better understanding.

Another possible explanation for the exposure of the starch granules on the surface could be that the micropyle zone allows the absorption of water for the physiological processes of the seed. During the cooking process, in addition to the progressive absorption of water, the micropyle can act as a carrier of some starch granules to the cooking water. Due to the presence of this starch (constituted by a high level of amylose (32–45.4%) and resistant starch (78.3%), beans are considered a low glycemic index food that attenuates the postprandial insulin response, which contributes to reduce colon cancer [72,83].

Elemental microanalysis of the seed coat surface in both samples (RBB and CBB) showed minerals such as Ca, K, Mg, Fe, Si, and Zn (Fig. 2e and f). The elemental analysis shows a decrease in the intensity of these minerals (Fig. 2d), highlighting CaOx crystals that are observed after seed rupture, which are found inside the multilayer tissue of the seed coat. This corroborates the decrease in ash content in CBB as shown in the proximate chemical analysis due to the diffusion of certain minerals in the cooking water.

Several studies have reported that beans are part of traditional diets in Mexico [84,85] and they are an important sources of iron,

zinc, and calcium. The surface of food matrices that have undergone cracking presents an irregular and complex texture that can be quantitatively characterized by parameters such as fractal dimension texture (FD_T) that allows analyzing the irregularities of the surface of an image and lacunarity (λ), which represents the distribution of the holes or "gaps" in an image [24,86]. A FD_T value of 2.4225 ± 0.0126 was obtained for RBB and 2.5371 ± 0.0174 for CBB according to Fig. 3a and b. The RBB image has a smooth surface that generated a relatively low FD_T value, which was also observed in the parameters of homogeneity and entropy. This smooth surface is given by the cuticle composed of hydrophobic substances (waxes), such as cutin and suberin [76]; this layer is partially solubilized by the cooking process, fracturing the surface of the MC cells and causing a crack pattern. The latter results in a higher FD_T value in CBB as the crack pattern provides a more complex surface, which generated rougher texture, greater entropy and homogeneity.

Lacunarity is a property of fractal objects that represents the distribution of holes or "gaps" in an image and is an indicator of the object's symmetry [24,87]. A λ value of 0.793 ± 0.043 for RBB and 0.233 ± 0.053 for CBB were obtained. RBB had higher values of lacunarity and a surface with less structures (Fig. 3c), therefore, the intensities of the pixels are lower, resulting in a greater space between each structure and a smoother surface. The CBB lacunarity value indicates that the cracking pattern on the seed surface filled the image in the same way throughout the scan (Fig. 3d), losing its smooth and compact structure. Similar results were obtained by Garcia-Armenta et al. [86], who found that the fracture pattern created by water penetration into the thick maltodextrin agglomerates influenced the homogeneity and symmetry of the surface.

3.2.3. *Atomic force microscopy*

Fig. 4 shows the topographic images of RBB and CBB obtained by AFM with a scan size of 2.5 × 2.5 μm^2 (Fig. 4). The RBB surface (Fig. 4a, b) corresponds to the cuticle that has a scaly and heterogeneous surface throughout the scanning area. As described in the ESEM images there is a solubilization of the cuticle and a cracking pattern induced by the cooking process, which generated clusters of macrosclereid cells, as seen in Fig. 4c depicting the CBB surface.

The circular surface of the macrosclereid cells can be seen throughout the image in Fig. 4d, with a diameter between 0.476 and 2.88 μm. Roughness parameters (R_a and R_q) showed significant differences in RBB and CBB. A R_a value of 53.37 ± 17.95 nm and R_q of 67.21 ± 60.97 nm was obtained for RBB, whereas a 50% increase in the values of R_a (121.67 ± 52.22 nm) and R_q (149.94 ± 22.58 nm) was observed after subjecting the bean to a cooking process.

After the cooking process the cuticle and minerals are partial solubilized and leaves the surface of the macrosclereid cells exposed, causing an increase in the roughness; in addition, the cooking process generates a pattern of cracking that contributes to the increase of the roughness in CBB.

The topographic images corroborate the morphological changes on the surface of RBB and CBB that are mainly attributed to the cracking pattern caused during the cooking process. AFM allowed observing quantitative changes in the roughness of beans subjected to a cooking process.

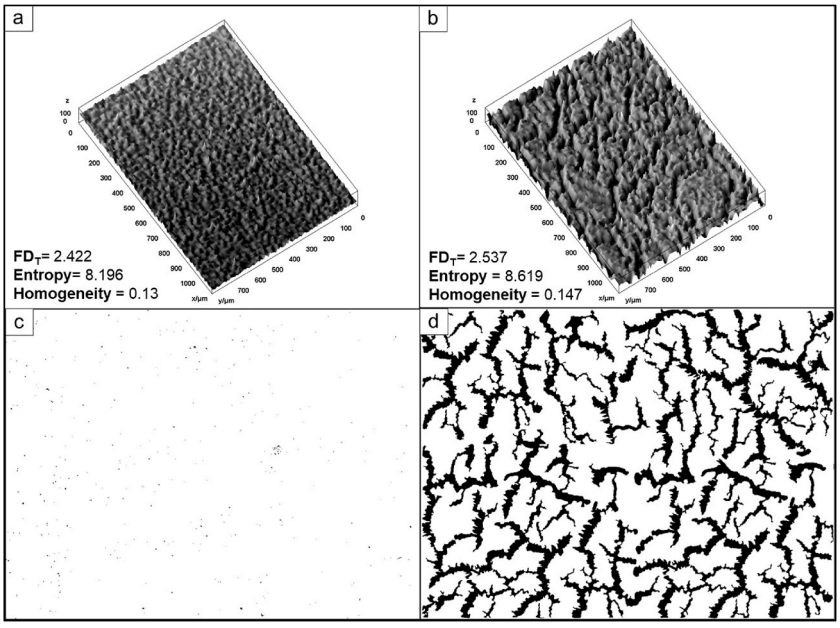

Fig. 3. FD_T values by the SDBC algorithm and 3D graph of the RBB (a) and CBB (b) surface, binary images of the RBB (c) and CBB (d) surface obtained by Image analysis from ESEM images.

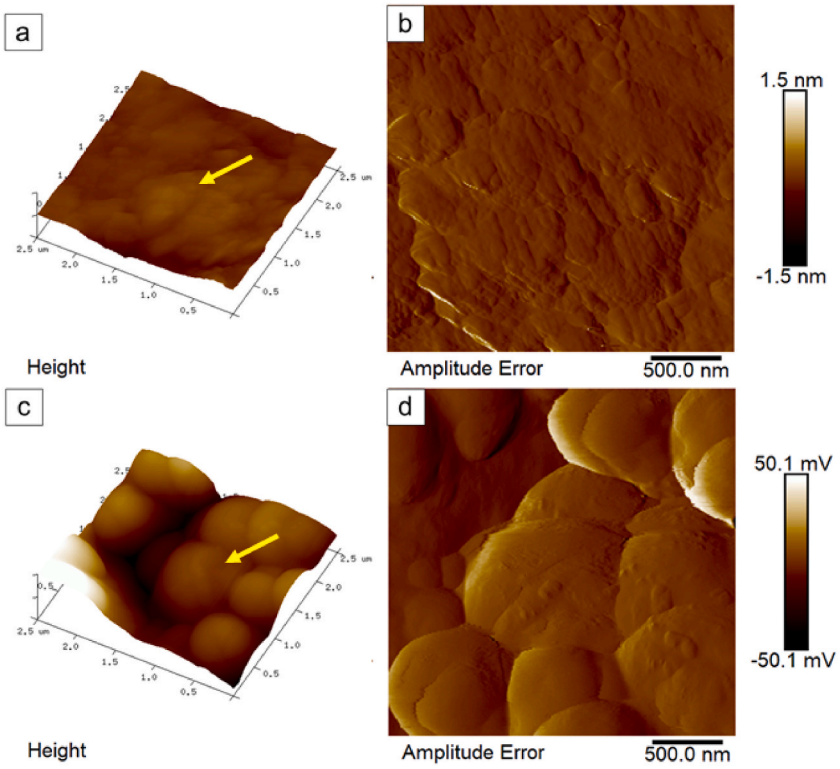

Fig. 4. AFM images of (a) height and (b) amplitude error from RBB and CBB (c, d), respectively. Scan size (2.5 × 2.5 μm^2).

3.3. Microstructural cross-sectional changes of the seed coat

3.3.1. ESEM characterization after the cooking process

Fig. 5 shows the images obtained by ESEM from a cross-section of the RBB and CBB, respectively. Fig. 5a shows the structure of the

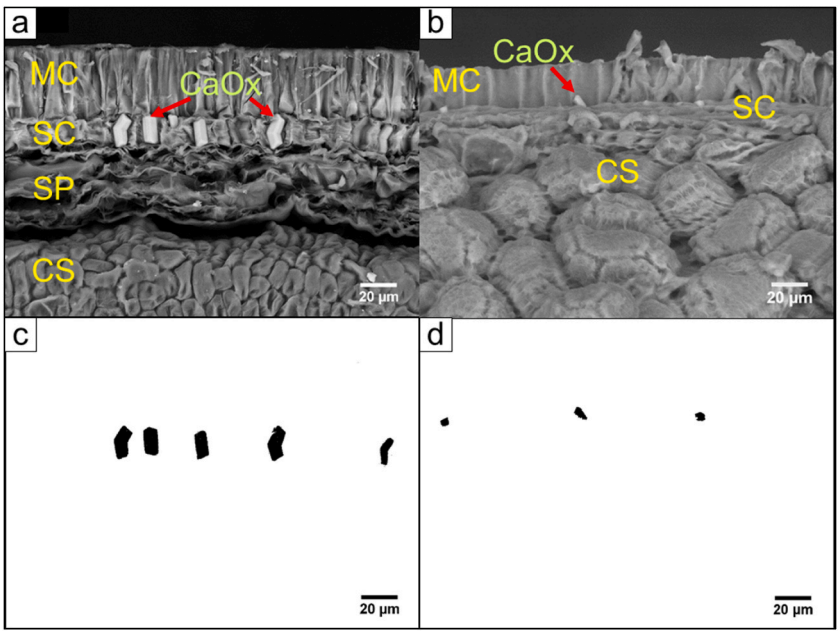

Fig. 5. ESEM images at 500× of RBB (a) and CBB (b), and their respective binary images (c) and (d). MC: Macrosclereid cells, SC: Subepidermal pillar cells, SP: Spongy parenchyma cells, CS: Cotyledon surface. CaOx: Calcium oxalate crystals.

different tissues of RBB: MC cells that make up the palisade tissue (38.97 μm), subepidermal pillar cells (SC) (17.21 μm), and spongy parenchyma cells (SP) (44.18 μm); then, the cotyledon surface (CS) is observed.

A decrease was observed in seed coat thickness after the cooking process because during this process the starch granules of the cotyledon initiate a swelling phenomenon that causes a rupture of the seed coat multilayer tissues, as shown in Fig. 5b. Individual CaOx crystals were found located inside the SC cells, which coincides with other studies [53,88] conducted on different biological materials, indicating that their production in the seed coat plays a protective role against insects.

During the cooking process (100 °C, 55 min), degradation of cell wall components occurred affecting the integrity of the multilayer walls, as has been reported for other legumes [82,89]. The bean grain expands 7% after cooking, generating a compression of the multilayer structure due to the swelling of the granules of the cotyledon, the SP zone is no longer spongy and elastic due to a reduction of its thickness, the SC cells decrease their size and number of CaOx crystals, losing rigidity. The MC cells are partially fractured and contribute together with the micropyle to promote water diffusion inside the grain.

Image analysis was carried out to evaluate the morphology of the CaOx crystals of RBB and CBB, from binary images show in Fig. 5c and d. The morphological features of crystals are shown in Table 1. The size parameters (A, P, Feret diameter) showed significant differences in RBB and CBB. These results indicate that the size of the CaOx crystals decreases in CBB, mainly due to the solubilization caused by the cracking of the seed by the cooking process.

The shape parameters of CaOx crystals were not significantly different between the samples. The values of the AR parameters of the oxalate crystals indicate their rectangular prism shape, these parameters serve as qualitative and quantitative indicators [90]. CaOx crystals can play several roles in plant tissues, such as protection, stiffness, and regulation of calcium content [91]. Structural changes during the cooking process in the seed coat multilayer affect the content of CaOx crystals in CBB.

3.3.2. Confocal laser scanning microscopy

Fig. 6 shows the optical and fluorescence images of a cross-section of RBB and CBB, where the different components that integrated the multilayer tissue of the seed coat and the main compounds of the endosperm, exposing the microstructural changes caused by the cooking process. Among the main changes observed in RBB (Fig. 6a) and CBB (Fig. 6c) are the decrease in size and abundance of CaOx crystals, swelling of SG. The cells forming the SP tissue leave abundant spaces among them to facilitate gas exchange, which after the cooking process is lost due to increased CS. The cell wall (CW) is found surrounding the bean cotyledon cells that contain the starch granules, the CW components (cellulose and hemicellulose) were evidenced by CLSM (Fig. 6b and d), where they were marked in blue,

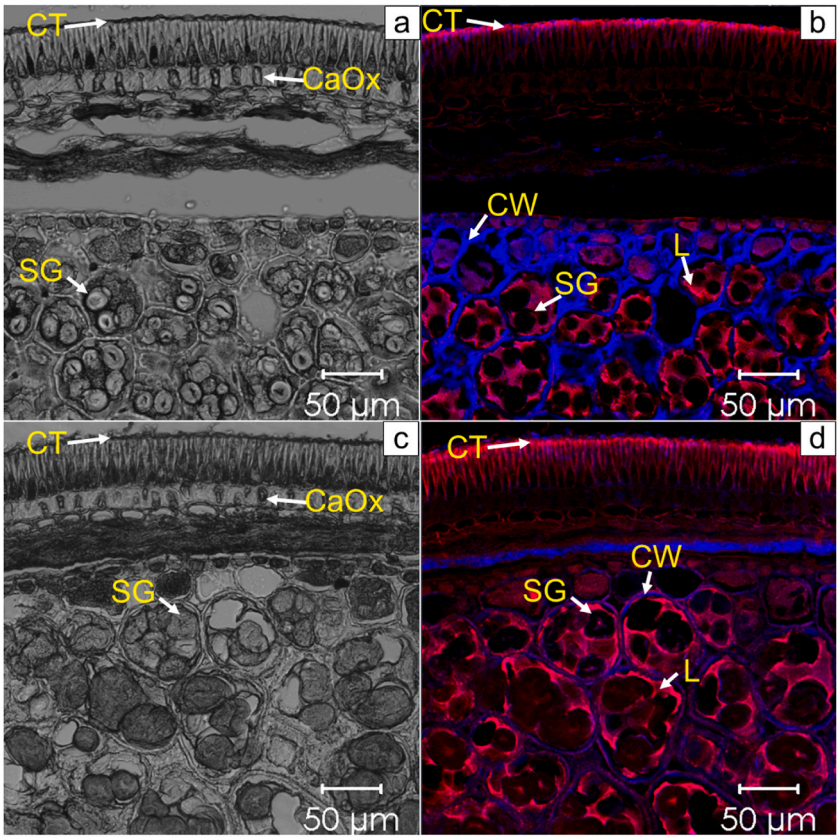

Fig. 6. Images obtained by CLSM of a cross-section of the sample. Optical image of RBB (a), calcofluor-Nile red stain of RBB (b), optical image of CBB (c) and its calcofluor-Nile red stain (d). SG: Starch granules; L: Lipids; CW: Cell wall; CT: Cuticle; CaOx: Calcium oxalate crystals

showing a decrease in CBB.

As previously described in the ESEM images, a swelling of the starch granules that could be covering the CW is observed and at the same time they are partially solubilized. This behavior can be explained from Fig. 6c, showing empty spaces where starch granules are observed inside the bean seed in the cotyledon structure of amyloplasts (Fig. 6a). Starch granules during the cooking process swell and lose their structural order, originating loss of the maltese cross (birefringence) (Fig. 6a–c) that has been described by Chaves Villareal et al. [92] and Chigwedere et al. [20]. It has been reported that seed coat permeability is low, so water is forced to enter through the raphe, hilum, and micropyle [82] during the cooking process, resulting in swelling of the starch granules. Pressure is exerted from the inside to the outside, causing the seed to expand, lose rigidity, the seed coat surface fracture, and granules migration into the cooking water.

Lipids are found around the SG and on the surface of RBB and CBB as evidenced by a red stain. Cuticle tissue is composed of hydrophobic substances (waxes), such as cutin and suberin [76] and the chromoplasts encrusted in the sclereids distributed in the MC cells [93].

Along the CBB cross-section (Fig. 6d), a red stain is observed in both the seed coat and the endosperm. The cell membranes of the different tissues constituting the seed have a membrane formed by a double layer of phospholipids. After the cooking process, this membrane breaks leaving exposed lipids, increasing their availability in the multilayer tissues of the seed coat and cotyledon as a consequence of the seed's cell expansion, which facilitates the formation of starch-lipid complexes [94] as evidenced by CLSM images.

In light of the results Fig. 7 presents a diagram that schematizes four main stages that characterize the cooking process. First (I): it begins with the solubilization of soluble compounds (proteins and minerals) on the surface of the seed coat, as observed in the chemical analysis and OM analysis. Second (II): the expansion of starch granules in the cotyledon by the cooking process exerts pressure from the inside to the outside, due to the progressive entry of water through the raphe, hilum, and micropyle. Third (III): The seed expands, loses rigidity, and gives rise to a compression of the multilayer structure of the seed coat that generates a cracking, forming clusters of MC cells on the surface, facilitating the entry of water into the cotyledon, and leading to the total swelling of the seed (7%). Fourth (IV): the softening of the starch granules generated the expansion of the cells, resulting in a greater availability of lipids in the seed coat and cotyledon, as evidenced by the CLSM images.

4. Conclusions and perspectives

The chemical composition, physical properties, the multilayer structure of the seed coat, and the morphological characteristics of the crystals in the studied beans were qualitatively and quantitatively affected by the cooking process. The distribution of minerals on the surface was determined by OM and the surface texture change was quantitatively characterized by the GLCM algorithm. The cooking process generated changes in the CBB surface as measured by the determination of fractal dimension parameters of texture and lacunarity. ESEM revealed cracking in the form of clusters in the cross section of bean seeds caused by the swelling of starch granules, as well as a decrease in the size of CaOx crystals quantified by morphological parameters (A, P, Feret diameter, and AR). AFM results revealed changes in seed coat surface topography that were quantitatively evidenced by roughness parameters (R_a and R_q). The lipid membrane, covering the seed coat and cotyledon cells, ruptured after the cooking process resulting in increased lipid availability, as evidenced by CLSM. The information provided by the techniques and methods allowed us to propose a model that explains the structural changes that take place in the bean by the cooking process, which consisted of four stages. The combination of microscopy techniques with image analysis contributes to a better understanding of the structural changes and their effect on the nutritional and functional properties induced by the cooking process. The data generated from this research offer data for the seed processing industries, since they allow the implementation of properly controlled cooking processes (parameters involved in the process, cook time, temperature, solid: liquid ratio, among others), which will reflect benefits in the quality of the final product.

Data availability statement

The data will be available on request.

Additional information

No additional information is available for this paper.

CRediT authorship contribution statement

Madeleine Perucini-Avendaño: Writing – original draft, Visualization, Validation, Methodology, Investigation, Formal analysis, Conceptualization. **Israel Arzate-Vázquez:** Writing – review & editing, Validation, Resources, Methodology, Conceptualization. **María de Jesús Perea-Flores:** Writing – review & editing, Visualization, Validation, Supervision, Resources, Methodology, Conceptualization. **Daniel Tapia-Maruri:** Resources, Methodology. **Juan Vicente Méndez-Méndez:** Validation, Resources, Methodology, Conceptualization. **Mayra Nicolás-García:** Writing – original draft, Visualization, Validation, Methodology, Investigation, Formal analysis, Conceptualization. **Gloria Dávila-Ortiz:** Writing – review & editing, Visualization, Validation, Supervision, Resources, Investigation, Funding acquisition, Conceptualization.

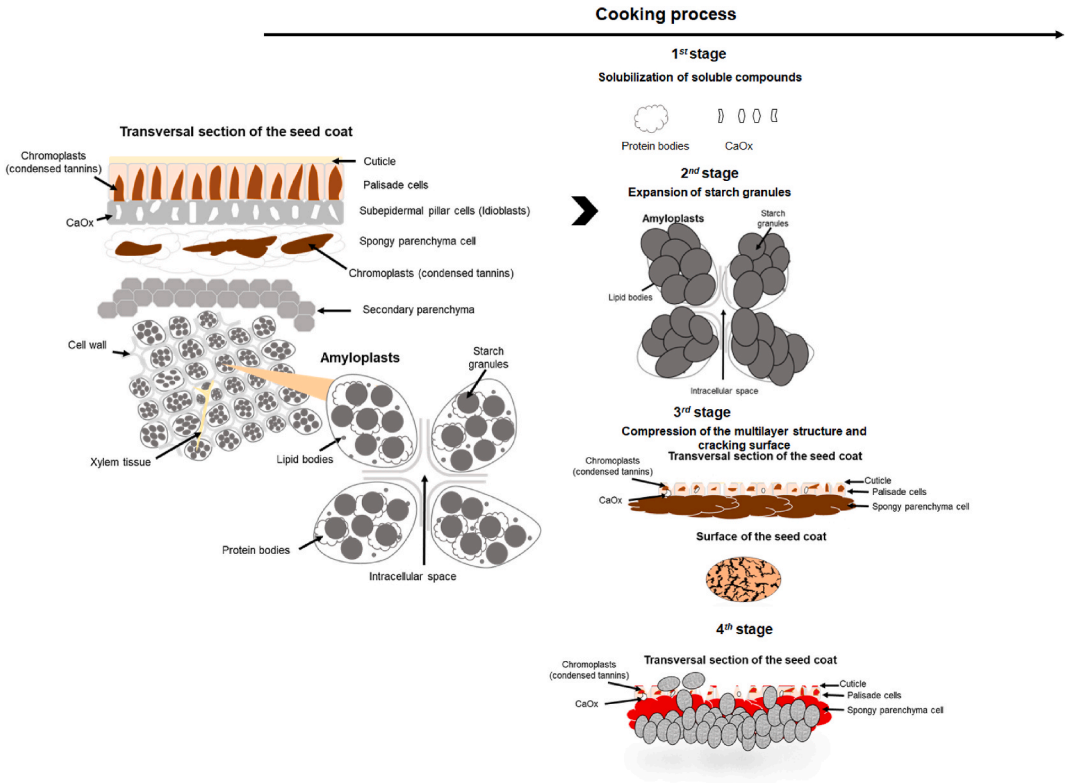

Fig. 7. Diagram of the microstructural changes by cooking process.

Declaration of competing interest

The authors declare that they have no known competing financial interests or personal relationships that could have appeared to influence the work reported in this paper.

Acknowledgements

The authors are grateful to the *Instituto Politécnico Nacional* (IPN Mexico) for the financial support provided through the SIP Projects (20181560, 20196640, and 20200291) and CONACyT projects (241756). Author M. Perucini-Avendaño acknowledges study grant from CONACYT-Mexico (590446). The authors also thank the *Centro de Nanociencias y Micro y Nanotecnología* (CNMN)-IPN and *Centro de Desarrollo de Productos Bióticos* (CEPROBI).

References

[1] Q.Q. Yang, R.Y. Gan, Y.Y. Ge, D. Zhang, H. Corke, Polyphenols in common beans (*Phaseolus vulgaris* L.): chemistry, analysis, and factors affecting composition, Compr. Rev. Food Sci. Food Saf. (2018), https://doi.org/10.1111/1541-4337.12391.

[2] D. Padilla-Chacón, C.B. Peña Valdivia, A. García-Esteva, M.I. Cayetano-Marcial, J. Kohashi Shibata, Phenotypic variation and biomass partitioning during post-flowering in two common bean cultivars (*Phaseolus vulgaris* L.) under water restriction, S. Afr. J. Bot. 121 (2019) 98–104, https://doi.org/10.1016/j.sajb.2018.10.031.

[3] F.G.B. Los, A.A.F. Zielinski, J.P. Wojeicchowski, A. Nogueira, I.M. Demiate, Beans (*Phaseolus vulgaris* L.): whole seeds with complex chemical composition, Curr. Opin. Food Sci. 19 (2018) 63–71, https://doi.org/10.1016/j.cofs.2018.01.010.

[4] Q.Q. Yang, R.Y. Gan, Y.Y. Ge, D. Zhang, H. Corke, Polyphenols in common beans (*Phaseolus vulgaris* L.): chemistry, analysis, and factors affecting composition, Compr. Rev. Food Sci. Food Saf. 17 (2018) 1518–1539, https://doi.org/10.1111/1541-4337.12391.

[5] F.G.B. Los, A.A.F. Zielinski, J.P. Wojeicchowski, A. Nogueira, I.M. Demiate, Beans (*Phaseolus vulgaris* L.): whole seeds with complex chemical composition, Curr. Opin. Food Sci. 19 (2018) 63–71, https://doi.org/10.1016/j.cofs.2018.01.010.

[6] N. Rocha-Guzmán, J. Gallegos-Infante, R. González-Laredo, A. Preza, Antioxidant Activity in Cotyledon of Black and Yellow Common Beans (*Phaseolus Vulgaris* L.).Pdf, 2014.

[7] A. Vargas-torres, P. Osorio-díaz, E. Agama-acevedo, L. Morales-franco, L.A. Bello-pérez, Digestibilidad del almidón en diferentes variedades de frijol (*Phaseolus vulgaris* L.), vol. 31, E.U.R.E.E. Re, 2006, pp. 881–884.

[8] R. Reynoso-Camacho, M. Ramos-Gómez, G. Loarca-Pina, Bioactive components in common beans (*Phaseolus vulgaris*), Adv. Agric. Food Biotechnol. (2006) 217–236.

[9] M. Ovando-Martínez, P. Osorio-Díaz, K. Whitney, L.A. Bello-Pérez, S. Simsek, Effect of the cooking on physicochemical and starch digestibility properties of two varieties of common bean (Phaseolus vulgaris L.) grown under different water regimes, Food Chem. 129 (2011) 358–365, https://doi.org/10.1016/j.foodchem.2011.04.084.

[10] E.R. Konzen, S.M. Tsai, Seed coat shininess in Phaseolus vulgaris: rescuing a neglected trait by its screening on commercial lines and landraces, J. Agric. Sci. 6 (2014), https://doi.org/10.5539/jas.v6n8p113.

[11] J. Nicolás-Bermúdez, I. Arzate-Vázquez, J.J. Chanona-Pérez, J.V. Méndez-Méndez, G.A. Rodríguez-Castro, H. Martínez-Gutiérrez, Morphological and micromechanical characterization of calcium oxalate (CaOx) crystals embedded in the pecan nutshell (Carya illinoinensis), Plant Physiol. Biochem. 132 (2018) 566–570, https://doi.org/10.1016/j.plaphy.2018.10.008.

[12] C. Chávez-Mendoza, E. Sánchez, Bioactive compounds from mexican varieties of the common bean (*Phaseolus vulgaris*): implications for health, Molecules 22 (2017), https://doi.org/10.3390/molecules22081360.

[13] M. Nicolás-García, I. Arzate-Vázquez, M. de J. Perea-Flores, J.V. Méndez-Méndez, M. Perucini-Avendaño, M.B. Gómez-Patiño, G. Dávila-Ortiz, An overview of instrumented indentation technique for the study of micromechanical properties in food: a case study on bean seed coat, Biosyst. Eng. 204 (2021) 377–385, https://doi.org/10.1016/j.biosystemseng.2021.02.006.

[14] F. Giusti, E. Capuano, G. Sagratini, N. Pellegrini, A comprehensive investigation of the behaviour of phenolic compounds in legumes during domestic cooking and in vitro digestion, Food Chem. 285 (2019), https://doi.org/10.1016/j.foodchem.2019.01.148.

[15] R. Nurzyńska-Wierdak, H. Łabuda, H. Buczkowska, A. Sałata, Pericarp of colored-seeded common bean (*Phaseolus vulgaris* L.) varieties a potential source of polyphenolic compounds, Agron. Res. 17 (2019), https://doi.org/10.15159/AR.19.187.

[16] C. Reyes-Moreno, Paredes-LapezOctavio, E. Gonzalez, Hard-to-cook phenomenon in common beans — a review, Crit. Rev. Food. Sci. Nutr. 33 (1993) 227–286, https://doi.org/10.1080/10408399309527621.

[17] A.C. Miano, J.A. García, P.E.D. Augusto, Correlation between morphology, hydration kinetics and mathematical models on Andean lupin (*Lupinus mutabilis* Sweet) grains, LWT - Food Sci. Technol. 61 (2015) 290–298, https://doi.org/10.1016/j.lwt.2014.12.032.

[18] P. Smýkal, V. Vernoud, M.W. Blair, A. Soukup, R.D. Thompson, The role of the testa during development and in establishment of dormancy of the legume seed, Front Plant Sci. 5 (2014) 1–19, https://doi.org/10.3389/fpls.2014.00351.

[19] A.C. Miano, E. Saldaña, L.H. Campestrini, A.F. Chiorato, P.E.D. Augusto, Correlating the properties of different carioca bean cultivars (*Phaseolus vulgaris*) with their hydration kinetics, Food Res. Int. 107 (2018) 182–194, https://doi.org/10.1016/j.foodres.2018.02.030.

[20] C.M. Chigwedere, T.F. Olaoye, C. Kyomugasho, Z. Jamsazzadeh Kermani, A. Pallares Pallares, A.M. Van Loey, T. Grauwet, M.E. Hendrickx, Mechanistic insight into softening of Canadian wonder common beans (*Phaseolus vulgaris*) during cooking, Food Res. Int. 106 (2018) 522–531, https://doi.org/10.1016/j.foodres.2018.01.016.

[21] M.J. Perea-Flores, J.J. Chanona-Pérez, V. Garibay-Febles, G. Calderón-Dominguez, E. Terrés-Rojas, J.A. Mendoza-Pérez, R. Herrera-Bucio, Microscopy techniques and image analysis for evaluation of some chemical and physical properties and morphological features for seeds of the castor oil plant (*Ricinus communis*), Ind. Crops Prod. 34 (2011) 1057–1065, https://doi.org/10.1016/j.indcrop.2011.03.015.

[22] M.V. irginia Mujica, M. Granito, N. Soto, Cambios microestructurales en los granos de *Phaseolus vulgaris* endurecidos, Arch. Latinoam. Nutr. 65 (2015) 110–118.

[23] V.A.G. Moran, Using Image Analysis Obtained by Scanning Electron Microscopy (SEM) for Determination of Sphericity in PVC Particles, 2011.

[24] E. García-Armenta, G.F. Gutiérrez-López, H. Hernández-Sánchez, L. Alamilla-Beltrán, Characterisation of the global breakage pattern of maltodextrin agglomerates, Powder Technol. 343 (2019) 362–365, https://doi.org/10.1016/j.powtec.2018.11.064.

[25] M. Nicolás-García, I. Arzate-Vázquez, M. de J. Perea-Flores, J.V. Méndez-Méndez, M. Perucini-Avendaño, M.B. Gómez-Patiño, G. Dávila-Ortiz, An overview of instrumented indentation technique for the study of micromechanical properties in food: a case study on bean seed coat, Biosyst. Eng. 204 (2021) 377–385, https://doi.org/10.1016/j.biosystemseng.2021.02.006.

[26] J. Chanona-Pérez, R. Quevedo, A.R.J. Aparicio, C.G. Chávez, J.A.M. Pérez, G.C. Domínguez, L. Alamilla-Beltrán, G.F. Gutiérrez-López, Image processing methods and fractal analysis for quantitative evaluation of size, shape, structure and microstructure in food materials, in: G.F. Gutiérrez-López, G. V Barbosa-Cánovas, J. Welti-Chanes, E. Parada-Arias (Eds.), Food Engineering: Integrated Approaches, Springer New York, New York, NY, 2008, pp. 277–286.

[27] J. Nicolás-Bermúdez, I. Arzate-Vázquez, J.J. Chanona-Pérez, J.V. Méndez-Méndez, G.A. Rodríguez-Castro, H. Martínez-Gutiérrez, Morphological and micromechanical characterization of calcium oxalate (CaOx) crystals embedded in the pecan nutshell (*Carya illinoinensis*), Plant Physiology. Biochem. 132 (2018) 566–570, https://doi.org/10.1016/j.plaphy.2018.10.008.

[28] L.J. Corzo-Ríos, X.M. Sánchez-Chino, A. Cardador-Martínez, J. Martínez-Herrera, C. Jiménez-Martínez, Effect of cooking on nutritional and non-nutritional compounds in two species of *Phaseolus* (*P. vulgaris* and *P. coccineus*) cultivated in Mexico, Int. J. Gastron. Food Sci. 20 (2020) 100206, https://doi.org/10.1016/j.ijgfs.2020.100206.

[29] M. Dueñas, T. Sarmento, Y. Aguilera, V. Benitez, E. Mollá, R.M. Esteban, M.A. Martín-Cabrejas, Impact of cooking and germination on phenolic composition and dietary fibre fractions in dark beans (*Phaseolus vulgaris* L.) and lentils (*Lens culinaris* L.), LWT - Food Sci. Technol. 66 (2016) 72–78, https://doi.org/10.1016/j.lwt.2015.10.025.

[30] B. dos S. Siqueira, R.P. Vianello, K.F. Fernandes, P.Z. Bassinello, Hardness of carioca beans (*Phaseolus vulgaris* L.) as affected by cooking methods, LWT - Food Science and Technology 54 (2013) 13–17, https://doi.org/10.1016/j.lwt.2013.05.019.

[31] AOAC, The association of official analytical Chemists international, Off. Methods Anal. 38 (2016).

[32] M.A. Ortiz-Zarama, A.R. Jiménez-Aparicio, J. Solorza-Feria, Obtainment and partial characterization of biodegradable gelatin films with tannic acid, bentonite and glycerol, J. Sci. Food Agric. 96 (2016) 3424–3431, https://doi.org/10.1002/jsfa.7524.

[33] V.C. Shruti, M.P. Jonathan, P.F. Rodriguez-Espinosa, F. Rodríguez-González, Microplastics in freshwater sediments of Atoyac River basin, Puebla City, Mexico, Sci. Total Environ. 654 (2019) 154–163, https://doi.org/10.1016/j.scitotenv.2018.11.054.

[34] M.Q. Marin-Bustamante, J.J. Chanona-Pérez, N. Gvemes-Vera, I. Arzate-Vázquez, M.J. Perea-Flores, J.A. Mendoza-Pérez, G. Calderón-Domínguez, R.G. Casarez-Santiago, Evaluation of physical, chemical, microstructural and micromechanical properties of nopal spines (*Opuntia ficus-indica*), Ind. Crops Prod. 123 (2018) 707–718, https://doi.org/10.1016/j.indcrop.2018.07.030.

[35] N. Sharif, S. Khoshnoudi-Nia, S.M. Jafari, Confocal Laser Scanning Microscopy (CLSM) of Nanoencapsulated Food Ingredients, Elsevier Inc., 2020, https://doi.org/10.1016/b978-0-12-815667-4.00004-3.

[36] N. Singh, S.S. Jagwan, Seed Coat Structure in Bignoniaceae, vol. 1, 2009, pp. 121–124.

[37] R. Rai, A. Bhardwaj, S. Verma, Tissue fixatives: a review, Int. J. Pharmaceut. Drug Anal. 4 (2016) 183–187.

[38] A. Mansour, R. Chatila, N. Bejjani, C. Dagher, W.H. Faour, A novel xylene-free deparaffinization method for the extraction of proteins from human derived formalin-fixed paraffin embedded (FFPE) archival tissue blocks, MethodsX 1 (2014) 90–95, https://doi.org/10.1016/j.mex.2014.07.006.

[39] H. Jiang, M.C. Chen, Y.I. Lee, In vitro germination and low-temperature seed storage of Cypripedium lentiginosum P.J.Cribb & S.C.Chen, a rare and endangered lady's slipper orchid, Sci. Hortic. 225 (2017) 471–479, https://doi.org/10.1016/j.scienta.2017.07.040.

[40] I. Arzate-Vázquez, J.V. Méndez-Méndez, E.A. Flores-Johnson, J. Nicolás-Bermúdez, J.J. Chanona-Pérez, E. Santiago-Cortés, Study of the porosity of calcified chicken eggshell using atomic force microscopy and image processing, Micron 118 (2019) 50–57, https://doi.org/10.1016/j.micron.2018.12.008.

[41] I. Arzate-Vázquez, J.J. Chanona-Pérez, G. Calderón-Domínguez, E. Terres-Rojas, V. Garibay-Febles, A. Martínez-Rivas, G.F. Gutiérrez-López, Microstructural characterization of chitosan and alginate films by microscopy techniques and texture image analysis, Carbohydr. Polym. 87 (2012) 289–299, https://doi.org/10.1016/j.carbpol.2011.07.044.

[42] J. Rahimi, M.O. Ngadi, Structure and irregularities of surface of fried batters studied by fractal dimension and lacunarity analysis, Food Struct. 9 (2016) 13–21, https://doi.org/10.1016/j.foostr.2016.07.002.

[43] C. Isaza, K. Anaya, J.Z. de Paz, J.F. Vasco-Leal, I. Hernandez-Rios, J.D. Mosquera-Artamonov, Image analysis and data mining techniques for classification of morphological and color features for seeds of the wild castor oil plant (*Ricinus communis* L.), Multimed. Tools Appl. 77 (2018) 2593–2610, https://doi.org/10.1007/s11042-017-4438-y.

[44] P.K. Kinyanjui, D.M. Njoroge, A.O. Makokha, S. Christiaens, D.S. Ndaka, M. Hendrickx, Hydration properties and texture fingerprints of easy-and hard-to-cook bean varieties, Food Sci. Nutr. 3 (2015), https://doi.org/10.1002/fsn3.188.

[45] C.M. Chigwedere, D.M. Njoroge, A.M. Van Loey, M.E. Hendrickx, Understanding the relations among the storage, soaking, and cooking behavior of pulses: a scientific basis for innovations in sustainable foods for the future, Compr. Rev. Food Sci. Food Saf. (2019), https://doi.org/10.1111/1541-4337.12461.

[46] J.A.C. Bento, P.Z. Bassinello, R.N. Carvalho, M.A. de Souza Neto, M. Caliari, M.S. Soares Júnior, Functional and pasting properties of colorful bean (*Phaseolus vulgaris* L) flours: influence of the cooking method, J. Food Process Preserv. 45 (2021), https://doi.org/10.1111/jfpp.15899.

[47] M. Pujolà, A. Farreras, F. Casañas, Protein and starch content of raw, soaked and cooked beans (*Phaseolus vulgaris* L.), Food Chem. 102 (2007), https://doi.org/10.1016/j.foodchem.2006.06.039.

[48] S.H. Guzmán-Maldonado, J. Acosta-Gallegos, O. Paredes-López, Protein and mineral content of a novel collection of wild and weedy common bean (*Phaseolus vulgaris* L), J. Sci. Food Agric. 80 (2000), https://doi.org/10.1002/1097-0010(200010)80:13<1874::AID-JSFA722>3.0.CO;2-X.

[49] C. Miles, K.A. Atterberry, B. Brouwer, Performance of Northwest Washington heirloom dry bean varieties in organic production, Agronomy 5 (2015), https://doi.org/10.3390/agronomy5040491.

[50] J. Chen, X. Ren, Q. Zhang, X. Diao, Q. Shen, Determination of protein, total carbohydrates and crude fat contents of foxtail millet using effective wavelengths in NIR spectroscopy, J. Cereal Sci. 58 (2013), https://doi.org/10.1016/j.jcs.2013.07.002.

[51] H. Gardner, Lipid Enzymes: Lipases, Lipoxygenases, and "Hydroperoxidases,", 1980, https://doi.org/10.1007/978-1-4757-9351-2.

[52] J. Boye, F. Zare, A. Pletch, Pulse proteins: processing, characterization, functional properties and applications in food and feed, Food Res. Int. 43 (2010), https://doi.org/10.1016/j.foodres.2009.09.003.

[53] B. Finch-Savage, Seeds: physiology of development, germination and dormancy (3rd edition) - J.D. Bewley, K.J. Bradford, H.W.M. Hilhorst H. Nonogaki. 392 pp. Springer, New York – Heidelberg – Dordrecht – London2013978-1-4614-4692-7, Seed Sci. Res. 23 (2013), https://doi.org/10.1017/s0960258513000287, 289–289.

[54] S.M. Nasar-Abbas, J.A. Plummer, K.H.M. Siddique, P. White, D. Harris, K. Dods, Cooking quality of faba bean after storage at high temperature and the role of lignins and other phenolics in bean hardening, LWT 41 (2008), https://doi.org/10.1016/j.lwt.2007.07.017.

[55] C.D. Ferreira, V. Ziegler, R.T. Paraginski, N.L. Vanier, M.C. Elias, M. Oliveira, Physicochemical, antioxidant and cooking quality properties of long-term stored black beans: effects of moisture content and storage temperature, Int. Food Res. J. 24 (2017).

[56] A. Pallares Pallares, S. Rousseau, C.M. Chigwedere, C. Kyomugasho, M. Hendrickx, T. Grauwet, Temperature-pressure-time combinations for the generation of common bean microstructures with different starch susceptibilities to hydrolysis, Food Res. Int. 106 (2018) 105–115, https://doi.org/10.1016/j.foodres.2017.12.046.

[57] J.C. Ruiz-Ruiz, G. Dávila-Ortíz, L.A. Chel-Guerrero, D.A. Betancur-Ancona, Wet fractionation of hard-to-cook bean (*Phaseolus vulgaris* L.) seeds and characterization of protein, starch and fibre fractions, Food Bioproc. Tech. 5 (2012) 1531–1540, https://doi.org/10.1007/s11947-010-0451-0.

[58] D. Santiago-Ramos, J. de D. Figueroa-Cárdenas, J.J. Véles-Medina, R. Salazar, Physicochemical properties of nixtamalized black bean (*Phaseolus vulgaris* L.) flours, Food Chem. 240 (2018) 456–462, https://doi.org/10.1016/j.foodchem.2017.07.156.

[59] M. Himeda, N.N. Yanou, R.M. Nguimbou, C. Gaiani, J. Scher, J.B. Facho, C.M.F. Mbofung, Physicochemical, rheological and thermal properties of taro (*Colocassia esculenta*) starch harvested at different maturity stages, Int. J. Biosci. 2 (2012) 14–27.

[60] D. Perera, L. Devkota, G. Garnier, J. Panozzo, S. Dhital, Hard-to-cook phenomenon in common legumes: chemistry, mechanisms and utilisation, Food Chem. 415 (2023), https://doi.org/10.1016/j.foodchem.2023.135743.

[61] D. Chen, K. Hu, L. Zhu, M. Hendrickx, C. Kyomugasho, Cell wall polysaccharide changes and involvement of phenolic compounds in ageing of Red haricot beans (*Phaseolus vulgaris*) during postharvest storage, Food Res. Int. 162 (2022), https://doi.org/10.1016/j.foodres.2022.112021.

[62] D. Chen, U.T.T. Pham, A. Van Loey, T. Grauwet, M. Hendrickx, C. Kyomugasho, Microscopic evidence for pectin changes in hard-to-cook development of common beans during storage, Food Res. Int. 141 (2021), https://doi.org/10.1016/j.foodres.2021.110115.

[63] A.C. Telles, L. Kupski, E.B. Furlong, Phenolic compound in beans as protection against mycotoxins, Food Chem. 214 (2017), https://doi.org/10.1016/j.foodchem.2016.07.079.

[64] L.M.J. Carvalho, M.M. Corrêa, E.J. Pereira, M.R. Nutti, J.L.V. Carvalho, E.M.G. Ribeiro, S.C. Freitas, Iron and zinc retention in common beans (*Phaseolus vulgaris* L.) after home cooking, Food Nutr. Res. 56 (2012), https://doi.org/10.3402/fnr.v56i0.15618.

[65] C. Miglio, E. Chiavaro, A. Visconti, V. Fogliano, N. Pellegrini, Effects of different cooking methods on nutritional and physicochemical characteristics of selected vegetables, J. Agric. Food Chem. 56 (2008) 139–147, https://doi.org/10.1021/jf072304b.

[66] L.X. López-Martínez, N. Leyva-López, E.P. Gutiérrez-Grijalva, J.B. Heredia, Effect of cooking and germination on bioactive compounds in pulses and their health benefits, J. Funct. Foods 38 (2017) 624–634, https://doi.org/10.1016/j.jff.2017.03.002.

[67] H.M. Sánchez-Arteaga, J.E. Urías-Silvas, H. Espinosa-Andrews, E. García-Márquez, Effect of chemical composition and thermal properties on the cooking quality of common beans (*Phaseolus vulgaris*), CYTA - J. Food 13 (2015) 385–391, https://doi.org/10.1080/19476337.2014.988182.

[68] A.C. Miano, V.D. Sabadoti, P.E.D. Augusto, Enhancing the hydration process of common beans by ultrasound and high temperatures: impact on cooking and thermodynamic properties, J. Food Eng. 225 (2018) 53–61, https://doi.org/10.1016/j.jfoodeng.2018.01.015.

[69] E. Marconi, S. Ruggeri, M. Cappelloni, D. Leonardi, E. Carnovale, Physicochemical, nutritional, and microstructural characteristic of chickpeas (*Cicer arietinum* L.) and common beans (*Phaseolus vulgaris* L.) following microwave cooking, J. Agric. Food Chem. 48 (2000) 5986–5994, https://doi.org/10.1021/jf0008083.

[70] C.I. Teixeira-Guedes, D. Oppolzer, A.I. Barros, C. Pereira-Wilson, Impact of cooking method on phenolic composition and antioxidant potential of four varieties of *Phaseolus vulgaris* L. and *Glycine max* L, Lwt 103 (2019) 238–246, https://doi.org/10.1016/j.lwt.2019.01.010.

[71] A.P. Cárdenas-Castro, J. Pérez-Jiménez, L.A. Bello-Pérez, J. Tovar, S.G. Sáyago-Ayerdi, Bioaccessibility of phenolic compounds in common beans (*Phaseolus vulgaris* L.) after in vitro gastrointestinal digestion: a comparison of two cooking procedures, Cereal Chem. 97 (2020) 670–680, https://doi.org/10.1002/cche.10283.

[72] E. Chinedum, S. Sanni, N. Theressa, A. Ebere, Effect of domestic cooking on the starch digestibility, predicted glycemic indices, polyphenol contents and alpha amylase inhibitory properties of beans (*Phaseolis vulgaris*) and breadfruit (*Treculia africana*), Int. J. Biol. Macromol. 106 (2018) 200–206, https://doi.org/10.1016/j.ijbiomac.2017.08.005.

[73] A. Claudio, M. Pastor, Ultrasound assisted hydration of grains with sigmoidal behavior: kinetics of hydration, cooking, germination and nutrient incorporation University of Sao Paulo "Luiz de Queiroz" College of Agriculture Ultrasound assisted hydration of grains with sigm, 2019, https://doi.org/10.13140/RG.2.2.30794.21442.

[74] C. Chávez-Mendoza, K.I. Hernández-Figueroa, E. Sánchez, Antioxidant capacity and phytonutrient content in the seed coat and cotyledon of common beans (*Phaseolus vulgaris* L.) from various regions in Mexico, Antioxidants 8 (2019), https://doi.org/10.3390/antiox8010005.

[75] I. Arzate-Vaquez, Aplicación del análisis de textura de imágenes para la caracterización cuantitativa de superficies biológicas, 2011, p. 125.

[76] S. Shao, C.J. Meyer, F. Ma, C.A. Peterson, M.A. Bernards, The outermost cuticle of soybean seeds: chemical composition and function during imbibition, J. Exp. Bot. 58 (2007) 1071–1082, https://doi.org/10.1093/jxb/erl268.

[77] A. Mazur, The role of seed coat in the germination and early stages of growth of bean (Phaseolus vulgaris L.) in the presence of chickweed (Stellaria media (L.) Vill.), Annales Universitatis Paedagogicae Cracoviensis Studia Naturae (2019), https://doi.org/10.24917/25438832.4.6.

[78] N. Recek, M. Holc, A. Vesel, R. Zaplotnik, P. Gselman, M. Mozetič, G. Primc, Germination of *phaseolus vulgaris* l. Seeds after a short treatment with a powerful rf plasma, Int. J. Mol. Sci. 22 (2021), https://doi.org/10.3390/ijms22136672.

[79] C.I. Teixeira-Guedes, D. Oppolzer, A.I. Barros, C. Pereira-Wilson, Impact of cooking method on phenolic composition and antioxidant potential of four varieties of *Phaseolus vulgaris* L. and Glycine max L, Lwt 103 (2019) 238–246, https://doi.org/10.1016/j.lwt.2019.01.010.

[80] L. Fernández, C. Castillero, J.M. Aguilera, An Application of Image Analysis to Dehydration of Apple Discs, vol. 67, 2005, pp. 185–193, https://doi.org/10.1016/j.jfoodeng.2004.05.070.

[81] F. Mendoza, P. Dejmek, Colour and Image Texture Analysis in Classification of Commercial Potato Chips, vol. 40, 2007, pp. 1146–1154, https://doi.org/10.1016/j.foodres.2007.06.014.

[82] A.C. Miano, P.E.D. Augusto, The hydration of grains: a critical review from description of phenomena to process improvements, Compr. Rev. Food Sci. Food Saf. 17 (2018) 352–370, https://doi.org/10.1111/1541-4337.12328.

[83] B.P. Ávila, F.R. Nora, A.C. Pinto Seixas Neto, C.V. Rombaldi, L. da Silva Pinto, M.A. Gularte, M.C. Elias, Proteomic and physicochemical characteristics: the search for a quality profile of beans (*Phaseolus vulgaris* L.) during long-term storage, Lwt 133 (2020), https://doi.org/10.1016/j.lwt.2020.110057.

[84] S. Feitosa, R. Greiner, A.K. Meinhardt, A. Müller, D.T. Almeida, C. Posten, Effect of traditional household processes on iron, zinc and copper bioaccessibility in black bean (*Phaseolus vulgaris* L.), Foods 7 (2018) 1–12, https://doi.org/10.3390/foods7080123.
[85] C. Chávez-Mendoza, E. Sánchez, Bioactive compounds from mexican varieties of the common bean (*Phaseolus vulgaris*): implications for health, Molecules 22 (2017), https://doi.org/10.3390/molecules22081360.
[86] E. García-Armenta, D.I. Téllez-Medina, L. Alamilla-Beltrán, H. Hernández-Sánchez, G.F. Gutiérrez-López, Morphometric analysis of transverse surface of fractured maltodextrin agglomerates, Int. J. Food Prop. 19 (2016) 2451–2462, https://doi.org/10.1080/10942912.2015.1136940.
[87] N.A. Valous, F. Mendoza, D.W. Sun, P. Allen, Texture appearance characterization of pre-sliced pork ham images using fractal metrics: fourier analysis dimension and lacunarity, Food Res. Int. 42 (2009) 353–362, https://doi.org/10.1016/j.foodres.2008.12.012.
[88] R.B.N. Prasad, Walnuts and Pecans, Encyclopedia of Food Sciences and Nutrition, second ed., 2003, pp. 6071–6079, https://doi.org/10.1016/B0-12-227055-X/01269-4.
[89] M. Nicolás-García, M. Perucini-Avendaño, C. Jiménez-Martínez, M. de J. Perea-Flores, M.B. Gómez-Patiño, D. Arrieta-Báez, G. Dávila-Ortiz, Bean phenolic compound changes during processing: chemical interactions and identification, J. Food Sci. 86 (2021) 643–655, https://doi.org/10.1111/1750-3841.15632.
[90] A. Mazzoli, G. Moriconi, Particle size, size distribution and morphological evaluation of glass fiber reinforced plastic (GRP) industrial by-product, Micron 67 (2014) 169–178, https://doi.org/10.1016/j.micron.2014.07.007.
[91] P.A. Nakata, Ad V Ances in Our Understanding of Calcium Oxalate Crystal Formation and Function in Plants, 2003, p. 164, https://doi.org/10.1016/S0168-9452(03)00120-1.
[92] Claudia Chaves Villarreal, Allen Puente, Evaluación de las técnicas SEM y EDS para la investigación nanotecnológica de catalizadores para la producción de biocombustibles, 2013, p. 35.
[93] J.G.A. Whitehill, H. Henderson, M. Schuetz, O. Skyba, M.M. Saint Yuen, J. King, A.L. Samuels, S.D. Mansfield, J. Bohlmann, Histology and cell wall biochemistry of stone cells in the physical defence of conifers against insects, Plant Cell Environ. 39 (2016) 1646–1661, https://doi.org/10.1111/pce.12654.
[94] S. Wang, C. Chao, J. Cai, B. Niu, L. Copeland, S. Wang, Starch–lipid and starch–lipid–protein complexes: a comprehensive review, Compr. Rev. Food Sci. Food Saf. 19 (2020) 1056–1079, https://doi.org/10.1111/1541-4337.12550.